DOI: 10.1002/chem.200903076

Car–Parrinello Molecular Dynamics Study of the Thermal Decomposition of Sodium Fulminate

Konstantina Damianos and Irmgard Frank*[a]

Abstract: Depending on the metal cation, metal fulminates exhibit a characteristic sensitivity with respect to heat and mechanical stress. In the present paper we study the high-temperature reactions of bulk sodium fulminate using Car–Parrinello molecular dynamics simulations. We find that the initiating reaction is the formation of the fulminate dimer, while in earlier studies an electron transfer was assumed to be the first reaction step. The initial carbon–carbon bond formation is followed by fast consecutive reactions leading to polymerisation. The resulting species remain charged on the timescale of the simulations.

Keywords: energetic materials · fulminates · molecular dynamics · polymerization · reaction mechanisms

Introduction

Nowadays there is enormous interest in energetic materials with a wide range of civil, military and space applications.[1,2] These materials are divided into two main categories, namely the propellants and the detonating explosives. Propellants may react in a controlled manner and create high gas pressures which can be used to move vehicles, rockets and projectiles. Explosives react violently and are used in construction, mining, tunneling operations and warfare, but also in pyrotechnics. They can further be categorised in primary and secondary explosives, depending on their sensitivity with respect to heat, friction, impact and mechanical stress. Primary explosives, for example fulminates and azides, are very sensitive and detonate immediately whereas secondary explosives such as TNT and HMX, are less sensitive and can be transported and handled more easily. Present developments aim at propellants and explosives with higher performance, greater detonation velocities and more environmentally friendly behaviour.[3–5] In spite of this practical relevance only few theoretical studies exist addressing the reaction mechanism. This little theoretical knowledge is also surprising in view of the fact that many of these systems represent well-known text book chemicals.[6] More attention was paid to the kinetics of the reactions.[7–9] In addition, the crystal structures of fulminates were investigated in recent studies.[10–12] For these compounds it is known that the degree of covalency determines the immediacy of the decomposition.[13] Kinetic studies have shown that the ionic alkaline fulminates, alkaline earth fulminates, and thallous fulminate are prone to instant one-step explosions showing relatively high propagation velocities. In contrast, for the covalent mercury fulminate a preliminary burning stage precedes the explosion.[7,13] The reactions of the covalent solids have also been described as catalysed reactions.[14] Spectroscopic analysis before and after decomposition showed an increase in the vibrational frequencies of the carbon-nitrogen bond for the ionic fulminates, which was related to the formation of linear $C_nN_oO_p$ chains. In contrast, for covalent fulminates a decrease in these frequencies was explained by a cluster formation ($M_nC_nN_oO_p$).[7,15] The gaseous products carbon monoxide, carbon dioxide, nitrogen, and metallic vapour were observed for both types of fulminates. In addition, cyanate was found for the ionic fulminates.[7,10,16]

For the ionic solid of sodium fulminate in particular, the mechanism is unclear. The substance decomposes spontaneously above 500 K. Tentatively, the following reaction steps have been proposed:[7]

$$n\,CNO^- \rightarrow n\,CNO + n\,e^- \quad (1)$$

$$n\,CNO \rightarrow (CNO)_n \rightarrow \text{complex product} + p\,CO_2 + q\,CO + r\,N_2 \quad (2)$$

[a] K. Damianos, Prof. Dr. I. Frank
Fachgebiet Theoretische Chemie, Gottfried-Wilhelm-Leibniz Universität Hannover
Callinstrasse 3a, 30167 Hannover (Germany)
E-mail: irmgard.frank@theochem.uni-hannover.de

Supporting information for this article is available on the WWW under http://dx.doi.org/10.1002/chem.200903076.

$$n\,Na^+ + n\,e^- \rightarrow n\,Na \qquad (3)$$

An electron transfer from the fulminate anions to the sodium cations was suggested to initiate the reaction. The activation energy, as calculated from kinetic data, was associated with this presumably rate-determining step of decomposition. According to this mechanism the remaining neutral CNO radicals polymerise to finally form the complex polymeric material, consisting of long, linear $C_nN_oO_p$ chains. The polymerisation step is believed to account for the explosive character of sodium fulminate. An electron transfer as described above from the anions to the metal cations is known for the decomposition of sodium azide.[9] During the decomposition of this related compound the continuous electron transfers to the sodium cations lead to a growth process by which the sodium atoms form large clusters. Nitrogen is finally formed, possibly from cleavage of the neutral diazide intermediate.[17] This mechanism is in perfect agreement with the experimental finding that azides with noble cations such as silver or copper are extremely reactive. One may doubt, however, that it applies to the fulminates since silver fulminate and mercury fulminate are less reactive than the highly explosive sodium fulminate.

In the present study we use Car–Parrinello molecular dynamics (CPMD) simulations to determine the reaction mechanism of the decomposition of sodium fulminate.[18–20] With this first-principles method the simultaneous motion of electrons and nuclei is described using the Car–Parrinello equations. All degrees of freedom are taken into account and the actual pathway of a chemical reaction is obtained as a result of the simulation. In previous work, we applied CPMD, for example, in the field of high-energetic materials to study the reaction between monomethylhydrazine and nitrogentetroxide (MMH/NTO), which is used as a propellant in rocket engines.[21,22] We found a variety of different reaction mechanisms, involving radical, acid–base, and redox chemistry. For sodium fulminate we again want to determine the most relevant reaction mechanisms, without specifying a certain reaction pathway or a specific type of chemical reactions in advance. Hence, we use the most intuitive way of accelerating chemical reactions, namely increasing the temperature until a reaction is observed on the picosecond time scale. Note that this simple approach works for highly reactive systems only. For reactions involving high barriers more targeted acceleration methods[23] are needed.

Results and Discussion

Bulk structure of sodium fulminate: The crystal structure of sodium fulminate is isomorphous with that of β-sodium azide.[24] The unit cell of the sodium fulminate crystal is rhombohedral with the cell constants $a = 4.95$ Å and $\alpha = 38°15'$. The structure resembles that of sodium azide which is given in ref. [25]. There is no experimental indication how the fulminate groups are ordered in the cell. Therefore, we chose two structures, one with alternating orientation of the fulminate groups (Figure 1a, supercell of the $R\bar{3}m$ structure) and one with all fulminate groups pointing in the same direction (Figure 1b, supercell of the $R32$ structure), see also the Supporting Information, Tables S1 and S2. We chose an orthorhombic supercell containing twelve NaCNO units. The size of this supercell is $6.47 \times 5.60 \times 13.75$ Å^3. The results of cell constant optimisations with the functionals LDA and BLYP are summarised in Table 1. The BLYP functional yields large deviations of as much as 18 percent for both structures. The LDA functional reproduces the cell constant a for both structures well with deviations in the order of one percent. The carbon–nitrogen and the sodium–oxygen distances are smaller than the experimental values whereby BLYP is closer to experiment for the intramolecular distan-

Table 1. Intra- and intermolecular distances for the two sodium fulminate bulk structures investigated. The geometries were fully optimised using the LDA and BLYP functionals as implemented in the CPMD program package. The structural data obtained with the LDA functional are in good agreement with experiment. The CN and NO distance and the distance between the Na and O planes are averaged over the twelve molecules in one supercell. Exptl, see ref. [24].

	Exptl	LDA	BLYP
bulk structure a)			
a [Å]	4.95	5.02	5.85
Δa [%]	–	1.41	18.18
r_{CN} [Å]	1.19	1.17	1.18
r_{NO} [Å]	1.40	1.25	1.29
d_{NaO} planes [Å]	1.08	0.79	1.24
ρ [g mL^{-1}]	2.60	2.47	1.57
bulk structure b)			
a [Å]	4.95	4.96	5.85
Δa [%]	–	0.20	18.18
r_{CN} [Å]	1.19	1.17	1.18
r_{NO} [Å]	1.40	1.25	1.28
d_{NaO} planes [Å]	1.08	0.87	1.25
ρ [g mL^{-1}]	2.60	2.57	1.57

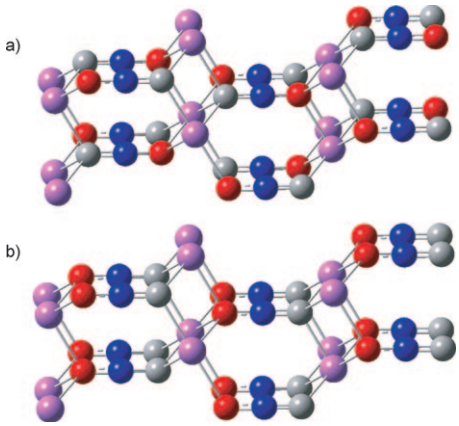

Figure 1. Two bulk structures of sodium fulminate with different orientations of the fulminate anions. Structure a): $R\bar{3}m$, structure b): $R32$. The supercell is orthorhombic with dimensions $6.47 \times 5.60 \times 13.75$ Å^3 and contains 12 NaCNO units. Color code: magenta: sodium; red: oxygen, blue: nitrogen, grey: carbon.

ces. Due to the better description of the intermolecular distances, we use the LDA functional for the high-temperature simulations of bulk structures in the following. For the simulation protocol see the section on Computational Details.

Molecular dynamics simulations: In five out of a total of seven simulations (two simulations at 700 and 900 K, respectively, showed no reactions at all) we obtain as the first reaction step the formation of a carbon–carbon bond of two fulminate anions leading to a dimer according to the following reaction scheme:

$$2\,CNO^- \rightarrow (CNO)^2_{2-}$$

The formed dimer is doubly negatively charged. The sodium atoms remain close to the dimer, but do not participate in any bond formation. No electron transfer from the fulminate groups to the sodium cations is observed. The electrons remain on the fulminate groups and are always paired. Depending on the initial orientation of the fulminate groups, the dimer may be formed in different isomers (having approximately C_{2v} or S_2 symmetry). These isomers exhibit the same reactivity in the consecutive reactions. The reaction continues either a) by condensation to the trimer, b) by isomerisation of the existing dimer, or c) by formation of a second dimer in the supercell:

$$(CNO)^2_{2-} + CNO^- \rightarrow (CNO)^3_{3-}$$

$$ONCCNO^{2-} \rightarrow NC(O)CNO^{2-}$$

$$2\,CNO^- \rightarrow (CNO)^2_{2-}$$

A polymerisation process is started, in which carbon–carbon atoms are repeatedly formed (Figure 2a). In addition, isomerisations take place within the oligomers leading to OCN^- units (Figure 2b) and $OCNO^-$ units (via a five-membered ring, Figure 2c). Cyanate anions are formed as byproducts (Figure 2d). Also a carbon–carbon bond cleavage may occur (Figure 2e). Finally, besides carbon–carbon bond formation also carbon–nitrogen bond formation is observed (Figure 2f). Snapshots from a simulation run which illustrate the isomerisation reactions are shown in Figure 3. The oligomers observed in the simulations have the general formula

$$C_nN_nO^n_{n-}$$

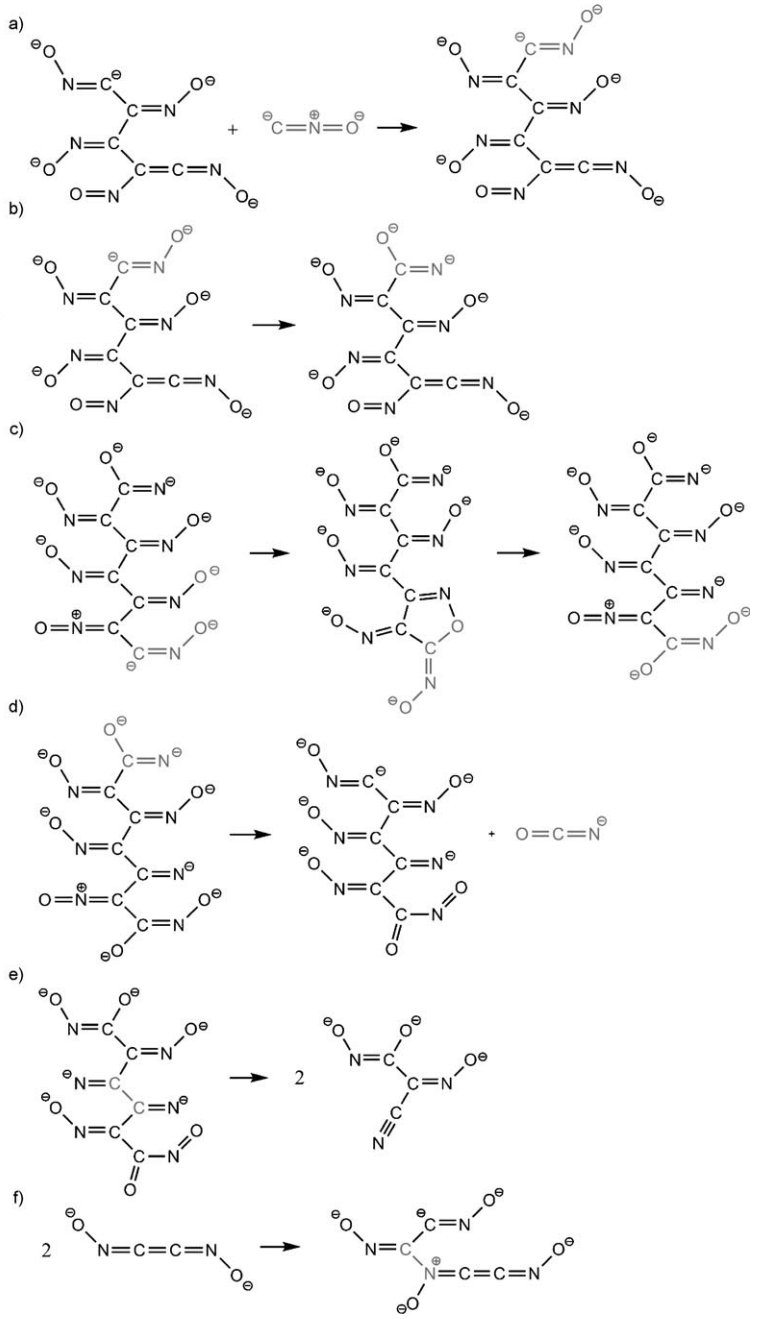

Figure 2. Characteristic reaction steps observed in high-temperature Car–Parrinello molecular dynamics simulations of sodium fulminate. Oligo- and polymerisation proceeds mostly by carbon-carbon bond formation a). Isomerisation reactions lead to the formation of OCN^- (b) and $OCNO^-$ groups (c). The possibility of carbon-carbon bond cleavage induces additional structural flexibility (d,e). To a minor extent, also carbon-nitrogen formation (f) is observed.

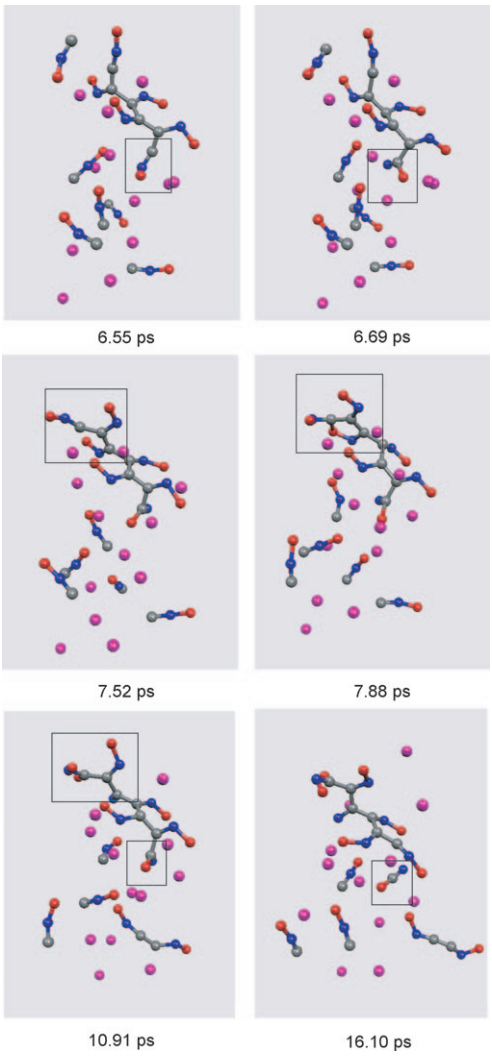

Figure 3. Snapshots from a Car–Parrinello molecular dynamics run. In the hexamer one of the CNO^- units isomerises to form an OCN^- group. An $OCNO^-$ group is formed via an intermediate containing a five-membered ring. The last snapshot shows the formation of a cyanate anion.

Further consecutive reactions may lead to different ratios of C, N, and O, but could not be observed on the timescale of the simulations. Formation of gaseous products such as carbonmonoxide is suppressed by the use of a constant volume in the simulations.

In the temperature range investigated, the reaction times for the initial dimer formation and for the consecutive reactions were in the range of a few picoseconds. The large spread and the small statistics do not allow a detailed analysis such, for example, an Arrhenius plot. The reaction rate seems to be dominated by entropic effects at the temperatures of the simulations with the enthalpic term playing only a minor role. In this regime the reaction times are more strongly influenced by the accidental arrangement of the reaction partners than by the actual temperature. The dimer formation (0.2–9.0 ps) and the consecutive reactions (0.8–16.7 ps) are essentially in the same time range for both structures. The particular arrangement of the anions (head-to-head or head-to-tail) in the bulk does not play an important role for the reactivity. This is not surprising in view of the fact that the structures were heated above the melting point of sodium fulminate. The dimerisation goes along with the melting of the structures. The limited simulation times do not allow observations of reactions at much lower temperatures. However, one would expect that also at lower temperatures the carbon–carbon bond formation will be the dominating reaction in the bulk, since the entropy is reduced in polymerisation reactions.

Static calculations: The determination of the energetics of the reactions observed in the simulations is hampered by the fact that the situation in the bulk is clearly different from the gas phase. This is particularly true for reaction barriers, but also for reaction energies. Gas-phase calculations can only give a crude estimate due to the dominant role of the Coulombic interaction between the charged particles in the bulk (see also ref. [22]). The particular arrangement of the ions influences the computed energies much stronger than do method and basis set. For example, the dimer (Figure 4a) can be isomerised to a ring of monomers (Figure 4b), which is more stable than the dimer by 1.56 eV. An alternative convention is to compute the energy differences between optimised educts and products (Figure 4) assuming infinitely distant educts. For this scenario, the polymerisation process is an exothermic reaction (BLYP/6-311++G(d,p)):

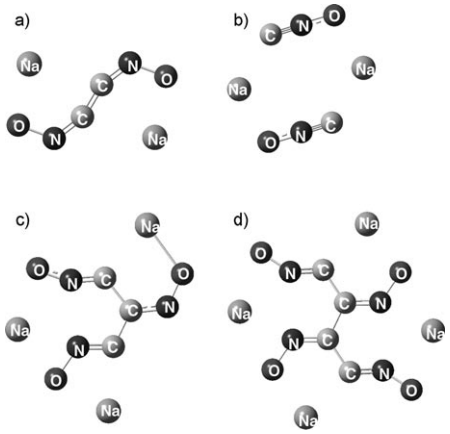

Figure 4. Optimised structures of the NaCNO dimer (a), trimer (c), and tetramer (d), and of a ring-shaped arrangement of two NaCNO monomers (b) (BLYP/6-311++G(d,p)).

$$2\ \mathrm{NaCNO} \rightarrow \mathrm{Na_2(CNO)_2},\ \Delta E = -0.48\ \mathrm{eV} \quad (4)$$

$$3\ \mathrm{NaCNO} \rightarrow \mathrm{Na_3(CNO)_3},\ \Delta E = -2.23\ \mathrm{eV} \quad (5)$$

$$4\ \mathrm{NaCNO} \rightarrow \mathrm{Na_4(CNO)_4},\ \Delta E = -3.67\ \mathrm{eV} \quad (6)$$

The exothermicity per NaCNO molecule grows with increasing chain length which successively leads to more stable

products. However, since the positioning of the sodium atoms strongly influences the calculated energies, these gas-phase calculations just give a crude estimate of the energetics in a solid material. As the low energy of the ring of two monomers indicates, an ordered arrangement of anions and cations is stabilised by the Coulombic force and hence may prevent fulminate polymerisation. Static calculations have been carried out for the isomerisation of the fulminate anion CNO^- to the cyanate anion OCN^- via a three-membered ring. This isomerisation has been discussed as the mechanism for cyanate formation and was investigated before using DFT and coupled cluster methods.[26] To compare the performance of different functionals and basis sets, we did LDA and BLYP calculations using the CPMD program package (plane-wave basis set) and BLYP and B3LYP calculations using the Gaussian package (Gaussian basis set), see Figure 5. The shape of the potential energy curves

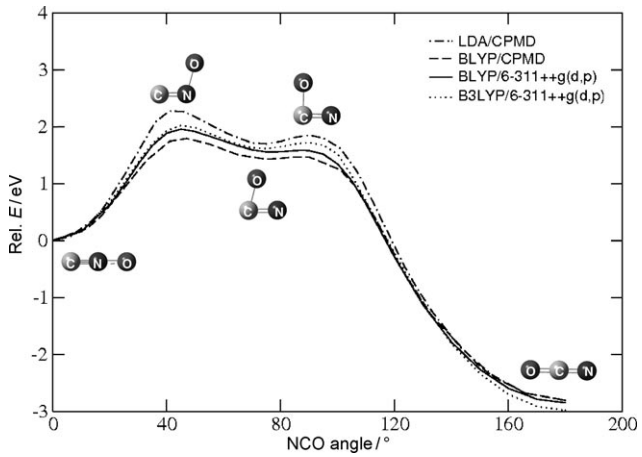

Figure 5. Potential energy curves for the isomerisation of CNO^- to OCN^-. The calculations were performed using the BLYP and B3LYP functionals with the 6-311++G(d,p) basis set, and the LDA and BLYP functionals with a plane wave basis set.

is the same for all approaches and the energy differences compare reasonably well to the data for the anionic species given in ref. [26] (CCSD(T)/aug-cc-pVDZ//B3LYP/6-31+G(d): 1.75 eV). We obtain reaction barriers in a range of 1.79 to 2.27 eV depending on method and basis set. The best numerical agreement with the coupled-cluster value is achieved with the BLYP functional and a plane wave basis set (1.79 eV). The larger plane-wave basis set tends to lower the barriers by about 0.1 eV. The computed barriers are too high to allow an ultrafast isomerisation via a three-membered ring and confirm the finding from the simulations, that the cyanate anion is rather formed by reactions involving several CNO^- units than by a three-ring isomerisation of the fulminate anion. In the bulk simulations we observe the formation of three-membered rings in CNO^- units that are part of an oligomer. In contrast to the isolated monomers, these units are already bent with CNO^- angles in the range of about 120 to 160°, which facilitates the isomerisation. (The Cartesian coordinates of the structures are given in the Supporting Information, Tables S3–S5.) As is shown in the reaction sequence in Figure 3, the isomerised group may easily dissociate to form a stable OCN^- cation. This reaction sequence offers a more favourable pathway for cyanate formation.

Conclusion

We simulated the first reaction steps for the thermal decomposition of bulk sodium fulminate and observed as the initiating reaction the formation of the fulminate dimer. We did not observe, however, an electron transfer from the fulminate anion to the sodium cations as proposed in the literature on the basis of the comparison to the decomposition of azides. An ionic mechanism is in line with the notion that ionic fulminates are extremely reactive in contrast to ionic azides. Also, the carbon–carbon dimerisation can be expected to be less effective if the carbon atoms are already coordinated to a metal cation, as is the case in mercury fulminate and silver fulminate. The initial dimerisation is quickly followed by polymerisation and isomerisation steps which ultimately lead to the formation of ionic oligomers. Our finding that the decomposition is initiated by a carbon–carbon bond formation followed by fast consecutive reactions, appears to be in nice agreement with the sensitivity of fulminates with respect to mechanical load and with the fast one-step decomposition observed in experiment.[13]

Beyond the timescale which is accessible to first-principles simulations, additional processes will occur besides the prolongation of the oligomers. A clustering of the sodium cations in conjunction with neutralising electron transfers will become favourable as the polymer gets longer and highly charged. Particularly at surfaces and grain boundaries, which are not modelled in our simulations, gaseous products such as carbon monoxide will be formed, inducing the actual explosion. As a result the chemical composition of the remaining polymer will differ from the total formula $(CNO)^{n-}_n$ obtained in the simulations which only describe the first few picoseconds of the bulk reaction.

The present study demonstrates once more the strong limitations of conventional static calculations in the description of condensed phase reactions. The use of reactive molecular dynamics is essential in particular for the simulation of ionic mechanisms due to the dominating Coulombic interaction between ions.

Computational Details

We use density functional theory in the Kohn–Sham formulation[27,28] as implemented in the CPMD code.[20] A plane wave basis set is used with an energy cutoff of 70 Rydberg to describe the valence electrons. Troulliier-Martins pseudopotentials were used for the inner electrons.[29] For the simulations of the bulk structures, the unrestricted formulation of the LDA functional was chosen which gives a reliable description of the intermolecular distances in the bulk (see Table 1 and Supporting Informa-

tion, Table S6). The time step of the simulations is 4 a.u. (0.0968 fs). After equilibration, the system was quickly heated to the desired temperatures in the range between 700 and 1300 K and the simulations were continued at these temperatures for 58 ps (600 000 simulation steps). The simulations were performed using Nosé-Hoover thermostats for ions and electrons.[30,31] For the phonon spectrum and the fictitious kinetic energy of the electrons 2800 cm^{-1} and 0.028 a.u. were chosen, respectively. In addition, static calculations were performed with the functionals BLYP[32,33] and B3LYP[34] using the 6-311++G(d,p) basis set as implemented in the Gaussian 98 program package.[35]

Acknowledgements

We thank Wolfgang Beck for bringing this research subject to our attention. Financial support by the Deutsche Forschungsgemeinschaft (SFB 486, "Manipulation von Materie auf der Nanometerskala", SFB 749, "Dynamik und Intermediate molekularer Transformationen") is gratefully acknowledged.

[1] T. M. Klapötke, *Chemie der hochenergetischen Materialien*, de Gruyter, Berlin, **2009**.
[2] J. Akhavan, *The Chemistry of Explosives*, 2nd ed., RSC, Cambridge, **2004**.
[3] M. A. Hiskey, N. Goldman, J. R. Stine, *J. Energ. Mater.* **1998**, *16*, 119.
[4] M. B. Talawar, R. Sivabalan, M. Anniyappan, G. M. Gore, S. N. Asthana, B. R. Gandhe, *Combust. Explos. Shock Waves* **2007**, *43*, 62.
[5] G. Steinhauser, T. M. Klapötke, *Angew. Chem.* **2008**, *120*, 3376; *Angew. Chem. Int. Ed.* **2008**, *47*, 3330.
[6] A. F. Holleman, E. Wiberg, *Lehrbuch der Anorganischen Chemie*, de Gruyter, Berlin, **2007**.
[7] T. Boddington, Z. Iqbal, *Trans. Faraday Soc.* **1969**, *65*, 509.
[8] A. K. Galwey, M. E. Brown, *Thermal Decomposition of Ionic Solids*, Elsevier, Amsterdam, **1999**.
[9] G. B. Manelis, G. M. Nazin, Yu. I. Rubtsov, V. A. Strunin, *Thermal Decomposition and Combustion of Explosives and Propellants*, Taylor and Francis, London, **2003**.
[10] W. Beck, *Eur. J. Inorg. Chem.* **2003**, 4275.
[11] W. Beck, J. Evers, M. Göbel, G. Oehlinger, T. M. Klapötke, *Z. Anorg. Allg. Chem.* **2007**, *633*, 1417.
[12] W. Beck, T. M. Klapötke, *J. Mol. Struct.* **2008**, *848*, 94.
[13] F. P. Bowden, H. T. Williams, *Proc. R. Soc. London Ser. A* **1951**, *208*, 176.
[14] H. Rosenwasser, Report, US Army Engineer Research and Development Laboratories Fort Belvoir, Virginia, **1965**.
[15] V. P. Zhulanova, S. I. Bannov, V. M. Pugachev, S. M. Ryabykh, *High Energy Chem.* **2001**, *35*, 26.
[16] W. Beck, *Chem. Ber.* **1962**, *95*, 341.
[17] T. M. Klapötke, *J. Mol. Struct.* **2000**, *499*, 99.
[18] R. Car, M. Parrinello, *Phys. Rev. Lett.* **1985**, *55*, 2471.
[19] M. Parrinello, *Solid State Commun.* **1997**, *102*, 107.
[20] CPMD Version 3.11, J. Hutter, IBM Corporation **1990–2006**, MPI für Festkörperforschung, Stuttgart **1997–2001**.
[21] C. Nonnenberg, I. Frank, T. M. Klapötke, *Angew. Chem.* **2004**, *116*, 4686; *Angew. Chem. Int. Ed.* **2004**, *43*, 4586.
[22] C. Nonnenberg, I. Frank, *Phys. Chem. Chem. Phys.* **2008**, *10*, 4383.
[23] A. Laio, M. Parrinello, *Proc. Natl. Acad. Sci. USA* **2002**, *99*, 12562.
[24] Z. Iqbal, A. D. Yoffe, *Proc. R. Soc. London Ser. A* **1967**, *302*, 35.
[25] G. E. Pringle, D. E. Noakes, *Acta Crystallogr. Sect. B* **1968**, *24*, 262.
[26] S. Dua, J. H. Bowie, *J. Phys. Chem. A* **2003**, *107*, 76.
[27] P. Hohenberg, W. Kohn, *Phys. Rev. B* **1964**, *136*, 864.
[28] W. Kohn, L. J. Sham, *Phys. Rev. A* **1965**, *140*, 1133.
[29] N. Troullier, J. L. Martins, *Phys. Rev. B* **1991**, *43*, 1993.
[30] S. Nosé, *J. Phys. Condens. Matter* **1990**, *2*, SA115.
[31] W. G. Hoover, *Phys. Rev. A* **1985**, *31*, 1695.
[32] A. D. Becke, *Phys. Rev. A* **1988**, *38*, 3098.
[33] C. Lee, W. Yang, R. G. Parr, *Phys. Rev. B* **1988**, *37*, 785.
[34] A. D. Becke, *J. Chem. Phys.* **1993**, *98*, 5648.
[35] Gaussian 98, Revision A.6, M. J. Frisch, G. W. Trucks, H. B. Schlegel, G. E. Scuseria, M. A. Robb, J. R. Cheeseman, V. G. Zakrzewski, J. A. Montgomery, Jr., R. E. Stratmann, J. C. Burant, S. Dapprich, J. M. Millam, A. D. Daniels, K. N. Kudin, M. C. Strain, O. Farkas, J. Tomasi, V. Barone, M. Cossi, R. Cammi, B. Mennucci, C. Adamo, S. Clifford, J. Ochterski, G. A. Petersson, P. Y. Ayala, Q. Cui, K. Morokuma, D. K. Malick, A. D. Rabuck, K. Raghavachari, J. B. Foresman, J. Cioslowski, J. V. Ortiz, B. B. Stefanov, G. Liu, A. Liashenko, P. Piskorz, I. Komaromi, R. Gomperts, R. L. Martin, D. J. Fox, T. Keith, M. A. Al-Laham, C. Y. Peng, A. Nanayakkara, C. Gonzalez, M. Challacombe, P. M. W. Gill, B. Johnson, W. Chem, M. W. Wong, J. L. Andres, C. Gonzalez, M. Head-Gordon, E. S. Replogle, J. A. Pople, Gaussian, Inc., Pittsburgh, PA, **1998**.

Received: November 9, 2009
Published online: June 2, 2010

